Soft Matter

PAPER

View Article Online
View Journal | View Issue

Cite this: *Soft Matter*, 2023, **19**, 2637

Impact of mesogenic aromaticity and cyano termination on the alignment and stability of liquid crystal shells

Anjali Sharma, Rijeesh Kizhakidathazhath and Jan P. F. Lagerwall *

We carry out a strategic and systematic variation of the molecular structure of liquid crystals (LCs) molded into spherical shells, surrounded by aqueous isotropic phases internally and externally. Contrary to common expectation, based on previous studies that have almost exclusively been carried out with cyanobiphenyl-based LCs, we find that the director field aligns normal to the LC–water interface when we use an LC molecule that is entirely non-aromatic. We propose to explain this by the inability of such an LC to participate in hydrogen bonding, rendering the normal configuration favorable as it minimizes the molecular cross section in contact with the water. We also find that cyano-terminated LC molecules contribute greatly to stabilizing the LC–water interface. This explains why shells made of cyanobiphenyl LCs are much more stable than shells of LCs with non-cyano-terminated molecules, even if the latter exhibit aromatic cores. Unstable LC shells can be stabilized very efficiently, however, through the addition of a low concentration of molecules that are cyano-terminated, preferably below the threshold for dimerization. Our study provides a much clarified understanding of how the molecular structure dictates the stability and alignment of LC shells, and it will enable a diversification of LC shell research and applications to systems where the use of non-cyanobiphenyl LCs is required.

Received 12th January 2023,
Accepted 2nd March 2023

DOI: 10.1039/d3sm00041a

rsc.li/soft-matter-journal

1 Introduction

Microfluidics-produced liquid crystal (LC) shells, *i.e.*, double emulsions in which a thin spherical layer of liquid crystal is confined between internal and external isotropic phases,[1,2] constitute an exquisite platform for studying numerous intriguing physics phenomena related to, *e.g.*, spherical topology and topological defect configurations,[3–13] the balance between two- and three-dimensional ordering and between positive and negative curvature,[8,14,15] phase separation,[15,16] as well as peculiar optical phenomena.[17,18] They also hold potential for various applications, in particular when using elastomeric,[19,20] photoresponsive[21] or cholesteric liquid crystals.[22–25] Applied work generally requires the use of specific liquid crystal molecules (mesogens) that may be different from the typical research mesogens, to introduce new functionalities such as polymerizability,[26–30] or to tune key properties like refractive indices, birefringence, phase transition temperatures or helix pitch of cholesteric shells.[25,30]

This need exposes a great knowledge gap in the field, because almost all studies of liquid crystal shells have been made with a single class of mesogens, namely the popular cyanobiphenyl-based *n*(O)CB family, where *n* is the length of the single alkyl (CB)/alkoxy (OCB) chain, most often with $n = 5$ or $n = 8$, see Table 1. Mesogens typically consist of two distinctive units with antagonistic features:[31] (1) a rigid core comprising at least two cyclic hydrocarbons, often but not necessarily aromatic, sometimes carrying lateral substituents for tuning certain physical or chemical properties; (2) flexible terminal chains, usually alkyl or alkoxy chains, linked to the outside of the core. In case of rod-shaped mesogens, the chains are normally attached to the two ends, while for disc-shaped mesogens, the terminal chains are generally distributed around the circumference. The flexibility of the terminal chains, disrupting crystallization, balances the rigidity of the core, which promotes ordering. The relative lengths of chain and core, respectively, can shift this balance in either direction to promote the type of LC formation desired.

The *n*(O)CB class is actually quite unusual among mesogens, because these mesogens are highly asymmetric, with only one terminal chain, the other terminus being the highly polar cyano (also called nitrile) group. Moreover, the molecules tend to dimerize in an antiparallel fashion, arranging for maximum overlap of their aromatic regions.[33,34] Many mesogens of applied interest have no cyano group, for instance most reactive mesogens that are used for making liquid crystal elastomers (LCEs). The implications of the peculiarities of the *n*(O)CB mesogen class on LC shell behavior has hardly been

University of Luxembourg, Physics & Materials Science Research Unit, Luxembourg, Luxembourg. E-mail: jan.lagerwall@lcsoftmatter.com

Table 1 Mesogenic structure and (for mixtures) composition, phase sequence, dipole moment μ and relative permittivity along the director, $\varepsilon_{\parallel}$, for liquid crystals discussed in this paper. Data on phase sequence, μ and $\varepsilon_{\parallel}$ for 5CB, 8CB, 7OCB, MBBA, PCH-5 and CCH-5 are taken from ref. 32; for MPCC, μ was estimated in Avogadro. We were not able to find data on $\varepsilon_{\parallel}$ for M5N and MPCC

LC	Mesogen(s)	Phase sequence (°C)	μ (D)	$\varepsilon_{\parallel}$
5CB	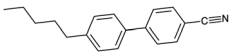	Cr. 24.0 N 35.3 Iso.	4.9–5.1	20 (25 °C, 1.5 kHz)
8CB	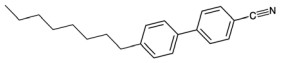	Cr. 21.5 SmA 33.5 N 40.5 Iso.	4.8–5.1	12.8 (34 °C)
7OCB	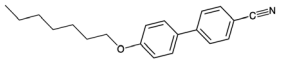	Cr. 53.5 N 75 Iso. Cr	4.9	15.0
MBBA	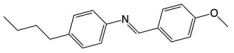	22.0 N 48.0 Iso.	3.2	4.7 (30 °C)
M5N	17.6 % 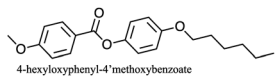 4-hexyloxyphenyl-4'methoxybenzoate 10.6 % 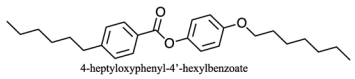 4-heptyloxyphenyl-4'-hexylbenzoate 24.3 % 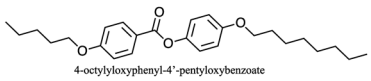 4-octylyloxyphenyl-4'-pentyloxybenzoate 27.5 % 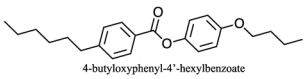 4-butyloxyphenyl-4'-hexylbenzoate 20.0 % 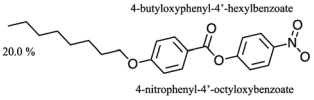 4-nitrophenyl-4'-octyloxybenzoate	Cr. <20 N 73.1–73.5 Iso.		
PCH-5	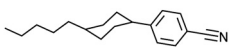	Cr 30.0 N 55.0 Iso.	4.1	14.4 (39 °C)
CCH-5	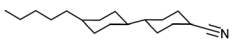	Cr 63.4 (Sm 40.5 SmB 49.1) N 86.4 Iso.	3.8	9.25 (73 °C)
MPCC	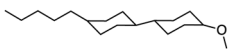	Cr. 28 N 38 Iso.	1.8	

investigated, but there are indications that the impact can be profound. For instance, in a recent study attempting to make LCE shells using a reactive mesogen without cyano group, we found that all shells broke almost immediately after production. However, by mixing in only 1 mol% of 7OCB, the shell stability was extended to many hours.[20]

Regardless of the scope and motivation of a study and regardless of which mesogens are used, ensuring stable liquid crystal–water interfaces and controlling the director alignment at these interfaces are crucial requirements. Both requirements are typically addressed by using different types of stabilizers, the classic choices being the water-soluble polymer polyvinylalcohol (PVA) for tangential alignment[35] and ionic surfactants for normal alignment.[36] Shells with tangential director field are recognized by textures such as those in Fig. 1(a)–(c) (from the top) or d (from the side). With normal alignment, the shell instead features a characteristic multi-ring texture with a Maltese cross, as shown in Fig. 1(e). Recently, several studies showed that the relationship between alignment and stabilizer can be more complex than previously realized. For instance, the alignment of shells stabilized by certain polymers may change upon approaching the transition to isotropic phase,[7,37] and surfactant-stabilized shells can show tangential and hybrid alignments (tangential alignment at one interface and normal at the other) if the concentration and/or chain length of surfactants is kept low.[14] Such observations may be compared with similar alignment transitions observed for LCs at solid interfaces, *e.g.*, near the transition to smectic or crystal in ferroelectric liquid crystals[38] or triggered by phase separation of polymers,[39] as well as in LC droplets, where a combination of additives promoting orthogonal alignment types can be used to dynamically tune the alignment.[40] Especially in the context of LC shells, the impact of the mesogen design itself on which alignment is obtained is a largely unexplored area.

In the present study, we try to fill these critical knowledge gaps, systematically exploring a number of non-*n*(O)CB mesogens in LC shell configuration, focusing on the shell stability and alignment in contact with aqueous PVA solutions in- and outside. We find that the cyano group indeed provides a significant stabilization of the shells, and, to our surprise, we find that the expected tangential alignment of a nematic phase in contact with water is replaced by normal alignment when using a mesogen with no aromatic group. The lack of further commercially available mesogens of this type and with suitable phase sequence prevents us from confirming the general validity of this observation, but we discuss how a lack of aromatic groups could explain the unexpected alignment. When mixing in 5CB to the non-aromatic LC at gradually increasing concentration, we find a step-by-step change from normal, *via* tilted, to tangential alignment, and a significant

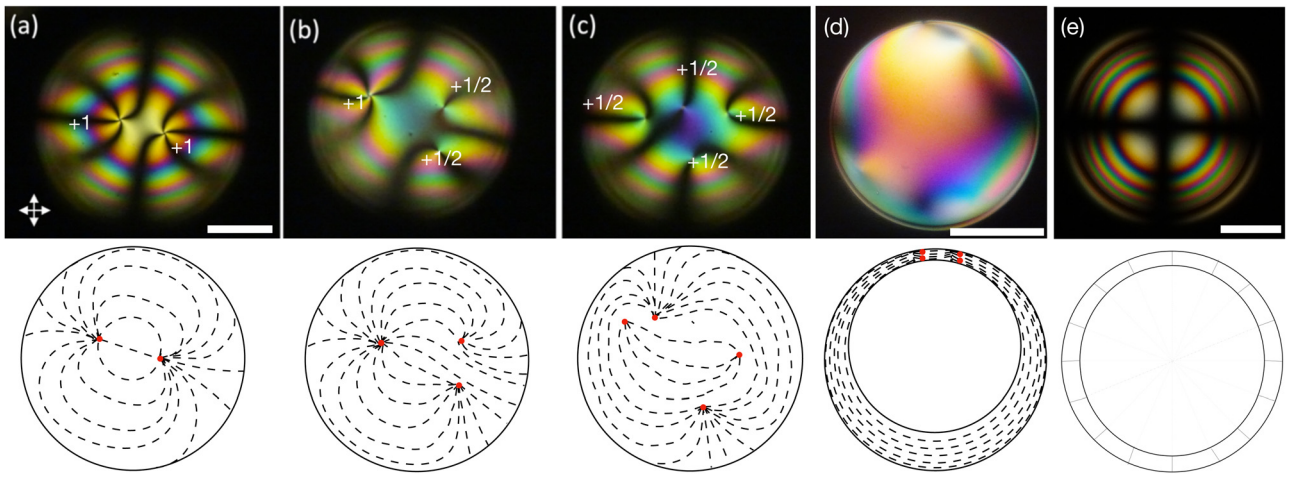

Fig. 1 Exemplary POM images (top row) of 5CB nematic shells with: tangential alignment seen from the top, focusing on the defect-containing thinnest part with (a) two +1 defects, (b) one +1 defect and two +1/2 defects, and (c) four +1/2 defects; (d) tangential alignment from the side, revealing the asymmetry with thin top and thick bottom; and (e) with normal alignment seen from the top (e). The bottom row shows schematic depictions of the corresponding director fields at (a)–(c) the thin top and (d), (e) in the central cross section. Note that the LC of the normal-aligned shell is defect-free. Scale bar: 100 μm.

stabilization of the shells in the first and last regimes, but not in the intermediate one.

2 Experimental details

2.1 Materials

An overview of all LCs considered here is provided in Table 1, listing their phase sequences as well as the structures, dipole moments and dielectric permittivities (when available). For reference, the table begins with 5CB and 8CB, both extensively studied in shell geometry, adding 7OCB as an example from the *n*OCB series. We then remove the cyano terminus while keeping the core aromatic, considering first the classic single-component nematogen *N*-(4-methoxybenzylidene)-4-butylaniline, commonly known as MBBA, which features a Schiff's base linking two phenyl rings. We also study a five-component mixture of mesogens with identical core of two ester-linked phenyl rings and varying non-cyano group termini, that we refer to as M5N. Next, we go back to the 5CB motif but remove one phenyl ring in PCH-5 (*trans*-4-(4-pentylcyclohexyl)benzonitrile) or both phenyl rings in CCH-5 (*trans*-4-(*trans*-4-*n*-pentylcyclohexyl)cyclohexylcarbonitrile), replacing them with aliphatic cyclohexanes. Finally, we consider the entirely non-aromatic mesogen MPCC (1-methoxy-4-(4-pentylcyclohexyl) cyclohexane), sharing a pentyl terminal group with 5CB, but the biphenyl is replaced by a bicyclohexane core, and the cyano group by a methoxy terminus.

The inner and outer phases are identical in all experiments, consisting of a 1 wt% aqueous solution of polyvinylalcohol PVA (M_w = 13–23 kg mol^{-1}, 87–89% hydrolyzed) from Sigma-Aldrich and dissolved in deionized water (resistivity 18 MΩ cm^{-1}, Sartorius arium pro-DI).

2.2 Methods

We produce shells using a coaxial glass capillary microfluidic device, with the LC as middle phase between the aqueous PVA solution used as outer and inner phases, as described in our previous work.[14] The capillary device is placed on a homemade temperature control plate placed on the stage of a Nikon Eclipse TS100 inverted microscope. The device is connected through thin, flexible polyethylene tubing to vials filled with PVA solution and the LC, and these vials are pressurized in a controlled way with a Fluigent MFCS system to initiate and regulate flow.

The production of LC shells is monitored and recorded using a high-speed camera (IDT NX4-S3) mounted on the microscope. After the production, we collect the shell suspension in a 2 ml glass vial. To investigate the shell textures we fill the suspension in a rectangular glass capillary and seal both ends, placing it in a Linkam T95-PE hot stage mounted on a Nikon Eclipse LV100ND polarizing optical microscope (POM). Images are captured using a Sony FDR AX33 camcorder, mounted on the microscope.

3 Results

3.1 Shells of LCs with mesogens with aromatic core but no cyano group

Our two LCs in this category are the single-component MBBA and the 5-component mixture M5N. To make shells of MBBA, we first heat the compound to 52 °C to ensure an isotropic state during production. Immediately after production, the shell suspension is filled into a flat glass capillary, which is transferred to the hot stage on the microscope, and then the shells are cooled to the nematic phase while observing the texture. We have to work fast, because the MBBA shells break after 30–40 minutes of production. After some annealing time, we see a texture[35] with four +1/2 topological defects (disclinations) near the thinnest point (the top) of the shell, see Fig. 2(a). This is one of the characteristic textures of tangential alignment, (Fig. 1(a)–(c)), the other comprising two +1/2 and one +1 defect, or two +1 defects.

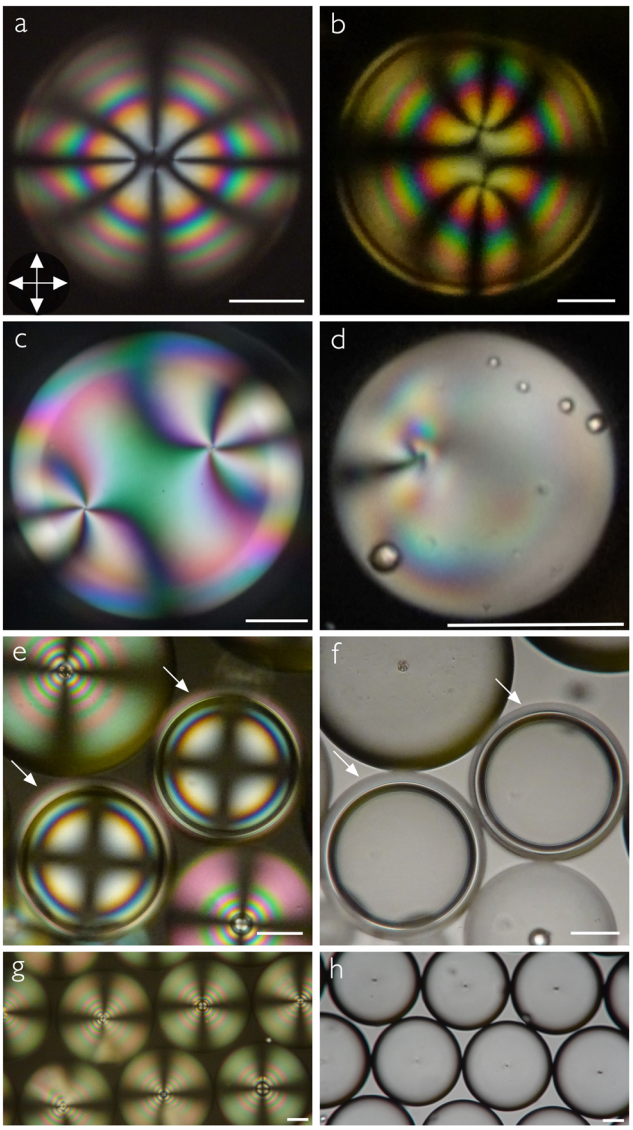

Fig. 2 POM images of shells of (a) MBBA (25 °C), (b) M5N (25 °C) and (c) PCH-5 (45 °C); a droplet of CCH-5 (d); and shells (e), (f) and droplets (g), (h) of MPCC between crossed polarizers (e), (g) and without analyzer (f), (h), at 30 °C. Crossed polarizers are aligned as the double arrows in (a). Scale bar in image (d) represent 50 μm and all other scale bars represent 100 μm.

Although one of them will typically be the equilibrium configuration—which one depends primarily on the thickness inhomogeneity[3]—all three can appear directly after shell production as the other two may be kinetically trapped.[7,37]

Doing the same experiment with the M5N mixture, this time producing the shells in the nematic phase at 50 °C, we again see shells with tangential alignment, as evidenced by the total +2 topological defect strength near the thinnest point, this time distributed over two +1 defects, see Fig. 2(b). While also hybrid-aligned shells exhibit textures with two +1 defects, they are easy to distinguish from those of tangential-aligned shells with two +1 defects, because in the latter case the defects aggregate close to the thinnest point of the shell (Fig. 1(a)), while in hybrid shells they are always at antipodal positions, one at the thickest and one at the thinnest point.[7,41,42] Also a tilted alignment, where the director is neither tangential nor normal to the interfaces with water, would be expected to have two +1 defects distributed over the shell, an issue we will come back to below. In that context, we will show that shells with tilted director have a texture that is distinctly different from tangential-aligned shells because of the broken symmetry with respect to the viewing direction. Considering all possible shell configurations with two +1 defects and their typical appearance, we can thus safely attribute the texture in Fig. 2(b) to tangential alignment.

The M5N shells are even less stable than those made with MBBA, breaking within 10 minutes of production. The low lifetime of both types of shells suggests that the absence of cyano-terminated mesogens reduces shell stability significantly. It thus appears that aromatic cores strongly promote tangential anchoring at the LC–aqueous interface, even without the cyano group terminus and even if the core is not a biphenyl but has a linking group between individual phenyl rings, but without the cyano termination the aromatic cores are not enough to provide good shell stability.

3.2 Shells and droplets of LCs with mesogens with cyano group and a single or no phenyl ring

We now attempt to prepare shells with PCH-5 and CCH-5, respectively. With PCH-5, shells are readily produced, and they again show the characteristic signature of tangential alignment in the nematic phase, the example in Fig. 2(c) having two +1 defects near its thinnest point. In contrast to the shells of MBBA and M5N, the PCH-5 shells have good stability, at least for several hours, such that we can cycle the temperature from the isotropic to deep nematic state and back several times without shell breaking.

Unfortunately, the more complex phase sequence of CCH-5, with a high melting point of 63.4 °C, monotropic higher-ordered phases (not fully characterized), and a clearing point of 86.4 °C, see Table 1, renders shell production of CCH-5 impractical: the aqueous phases would have to be heated too close to the boiling point for shell production to be possible. We therefore settle with studying droplets of this liquid crystal. The CCH-5 droplets are also tangentially aligned, albeit with a rather irregular texture, as shown in Fig. 2(d). The small bright spheres seen overlapping with the main droplet are most likely air bubbles, trapped during droplet production by vigorous shaking.

3.3 Shells of LCs with mesogens with non-aromatic core and without a cyano group

The shells prepared with MPCC are even less stable than those of MBBA and M5N and they often break during the initial observation right after production. Nevertheless, some shells survive long enough for us to confirm their texture, which surprisingly is entirely different from those of the previously studied LCs. The micrograph in Fig. 2(e) shows two shells (highlighted by white arrows) surrounded by droplets. The shell geometry is clear to see in panel (f), where the same sample is shown without analyzer. The shell texture shows no trace of

topological defects, but instead it looks qualitatively identical to the normal-aligned shell texture shown in Fig. 1(e). It characteristically combines a Maltese cross and a series of concentric rings, perfectly reminiscent of the conoscopy texture of flat LC samples with normal director (homeotropic alignment). As originally explained by Liang *et al.*,[41] normal-aligned LC shells observed in conventional (orthoscopic) POM appear this way because the optical situation is analogous to conoscopy of flat homeotropic samples: while in the latter case, all light directions are probed around a uniform optic axis, in the case of orthoscopic view of normal-aligned shells, all optic axis orientations are probed with uniform light direction. We can thus conclude that MPCC shells in contact with aqueous phases adopt a normal director field configuration, in stark contrast to conventional expectations.

Also the droplet texture is clearly that of normal boundary conditions, as shown in Fig. 2(g) for a large number of droplets. They all have a Maltese cross, reflecting the radial optic axis configuration within the droplet, as well as a bulk topological defect at the center, best seen in the micrograph obtained with focus on the equator plane of the droplets and without analyzer in Fig. 2(h). Note that the normal alignment of MPCC shells and droplets is different from the normal alignment that has been seen in *n*CB shells stabilized by block copolymer surfactants upon heating close to the clearing point:[7] those shells were always tangentially aligned well below the clearing point and they underwent a reversible alignment transition from tangential *via* hybrid to normal as the degree of orientational order is reduced on approaching the clearing point, most likely reflecting the reduction in anchoring strength at the interface to the aqueous block copolymer solution. In the case of MPCC shells, they are normal at any temperature studied, as are the droplets they convert into after breaking. We never saw any sign of tangential alignment for shells or droplets of pure MPCC, regardless of temperature.

This surprising behavior of MPCC shells and droplets suggests that an aromatic mesogen component is critical for obtaining tangential alignment of a well-developed nematic phase at an aqueous interface. Remarkably, already the minimum aromaticity provided by replacing the methoxy terminal group of MPCC with the cyano group in CCH-5 is enough to induce tangential alignment, as seen in Fig. 2(d). We will come back to suggesting an explanation for this behavior in the discussion, but first we explore the unusual alignment behavior of MPCC shells one step further. Because the cyano group seems to have such strong stabilizing character for shells, we explore if we can stabilize the MPCC shells by adding small amounts of a cyano-terminated mesogen, following the successful strategy for stabilizing LCE shells by Sharma *et al.*[20] We choose 5CB as our stabilizer additive, as this should maximize the tendency for the LC to adopt tangential alignment at the interface to the aqueous phase, creating an interesting frustration effect.

3.4 Stabilizing MPCC shells by mixing in 5CB

Adding small concentrations of 5CB, our hypothesis that the shells are stabilized by the *n*CB additive is confirmed: for both 1 wt% and 3 wt% 5CB we obtain shells that are stable for several days, and the alignment is unaffected by the 5CB, remaining normal as for pure MPCC, see Fig. 3. The texture of the very thin shells with 1 wt% 5CB contains some irregularities shortly after production, as seen in panel (a) obtained at 38 °C, just below the transition from the isotropic phase. Upon cooling to 25 °C a perfectly smooth normal texture develops. Because these shells are so thin, the Maltese cross is very broad at its center and there are no concentric rings; the entire shell is in the first order of birefringence. The shells with 3 wt% 5CB are more typical in thickness, exhibiting a correspondingly smaller cross and several rings visible near the shell perimeter.

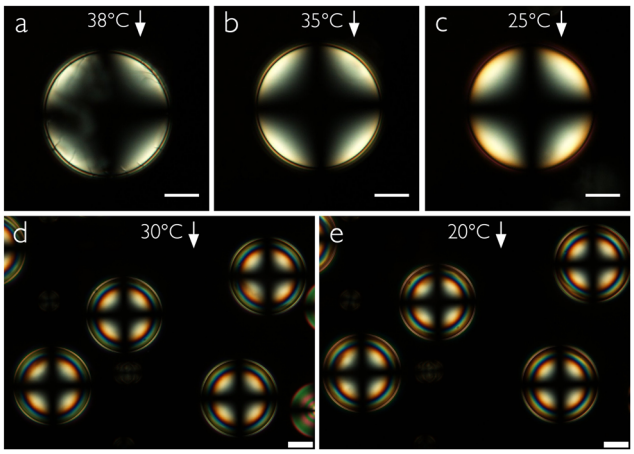

Fig. 3 (a)–(c) POM images of a normally aligned shell with 1 wt% 5CB + 99 wt% MPCC mixture at three different temperatures. (d), (e) Several shells with 3 wt% 5CB + MPCC mixture at two different temperatures, all showing normal alignment. Images are taken on cooling, in all cases with focus on the shell equator. Scale bar represents 50 μm.

Surprisingly, the stability increase is not a monotonic function of 5CB content: if we increase the 5CB content to 6 wt%, the shell stability decreases, all shells breaking within one hour. Moreover, the texture now reveals a tilted LC alignment at 30 °C, as recognized in Fig. 4(a) by an unusual texture that looks a bit like hybrid-aligned shells observed perpendicular to their symmetry axis.[8] The effective birefringence is greater towards the right in the figure, as seen by the colors traversing multiple orders in the Michel–Lévy diagram, while to the left it approaches zero, as seen by a distorted and highly off-center Maltese cross near the edge. This suggests that the director, and thus the optic axis, tilts from the shell normal, in a way that gives greater effective birefringence on the right than on the left side of the shell. A possible configuration is shown in Fig. 4(d), with the local director (equal to the optic axis) orientation within a cross section indicated with red lines. Assuming the same direction and magnitude of tilt throughout the shell cross section, we note that the top half shows maximum birefringence (horizontal director) when the bottom shows minimum birefringence (vertical director), and *vice versa*. Given the shell asymmetry with thick bottom and thin top, the effective color must be determined primarily by the director in the bottom half, hence the sketch in (d) seems appropriate for explaining the texture in (a).

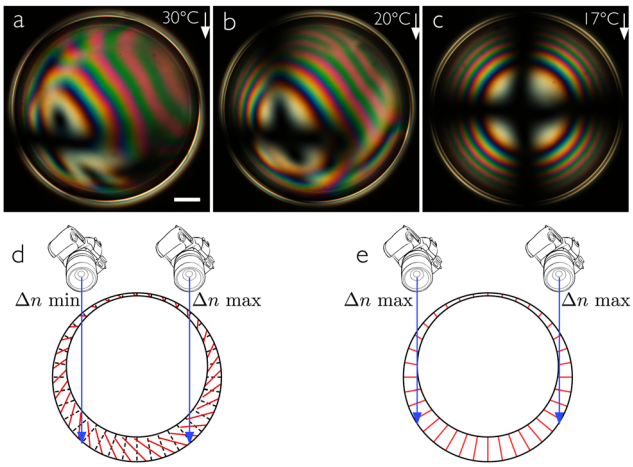

Fig. 4 POM images of a shell with 6 wt% 5CB + 94 wt% MPCC mixture. Image (a) shows tilted alignment in the shell. The alignment changes to normal on cooling (b), (c). In all photos the focus is on the shell equator. Scale bar represents 50 μm. Panel (d) illustrates how the increase in birefringence from left to right seen in (a) can be explained by a shell geometry with tilted director field, using red lines to indicate director and dashed black lines to indicate the radial direction. The classic normal-aligned shell geometry is shown in (e), giving maximum birefringence near the shell perimeter, corresponding to micrograph (c).

If the director tilts away from the normal direction, topological defects are unavoidable, because the tilting direction constitutes a tangential orientational field which, when mapped onto a sphere, must exhibit a total of +2 defects according to the Poincaré–Hopf theorem.[1,2] However, in contrast to a tangentially aligned shell, only integer defects are possible. This is because a 180° rotation around the shell normal is not a symmetry operation, since the tilting breaks the sign invariance of the global director field.[42] It is difficult to identify the defects in the textures in Fig. 4(a) and (b), and also upon focusing up and down through the shell the defects could not be detected. This is probably due to the complex optics of the tilted director field, but it could also be that the LC avoids the defect formation by gradually reducing the tilt locally to zero on approaching the points where the defects would otherwise have been. Such topologically driven local variations of the tilt magnitude would complicate the texture further, and it may be a reason why the total effective birefringence appears to go down to zero in at least one point in Fig. 4(a), which would not be expected from the simple director configuration in Fig. 4(d). On the other hand, this optical effect could also be explained by opposite directions of tilt at the top and bottom of the shell, which would be expected in case a +1 defect were located on the side of the shell, where it would be very difficult to detect.

Upon cooling the shell deeper into the nematic phase (Fig. 4(b) and (c)), the tilt reduces and a nearly regular normal-aligned shell texture is seen at 17 °C, corresponding to the director configuration sketched in Fig. 4(e). The change in the alignment between tilted and normal is reversible, the tilt reappearing if the shell is reheated. Comparing this with the temperature-dependent alignment change seen by Noh *et al.* in *n*CB shells stabilized by aqueous block copolymer solutions,[7] it is interesting to note that the alignment change direction is the opposite: heating these shells destabilizes their normal alignment, while heating the block copolymer-emulsified *n*CB shells destabilized their tangential alignment. Increasing the 5CB content to 10 wt%, the high-temperature alignment is tangential, see Fig. 5(a), but the stability is still poor. Moreover, on cooling, an alignment change is again seen, although it never reaches a fully normal configuration, but rather ends in a distorted transient state with a distinctive defect line, see Fig. 5(b) and (c) (further cooling leads to crystallization).

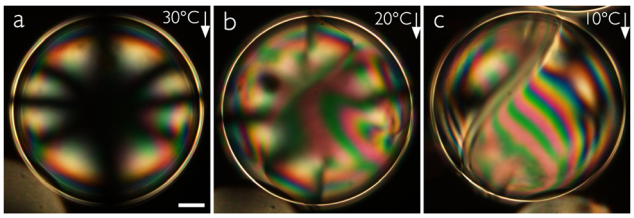

Fig. 5 POM images of a shell with 10 wt% 5CB + 90 wt% MPCC mixture. Images are taken on cooling (a: 30 °C; b: 20 °C; c: 10 °C), in all cases with focus on the shell equator. Scale bar represents 50 μm.

Interestingly, the shell stability is recovered if we further increase the 5CB concentration to 20 wt%. Now the shells are stable over several days, as for the shells with low concentration of 5CB, but this time we have entirely lost the normal alignment tendency. We study droplets as well as shells of this mixture, and no matter what temperature in the nematic phase we study (we cool down to 1 °C), they are tangentially aligned, see Fig. 6. Droplets show a bipolar defect arrangement characteristic of

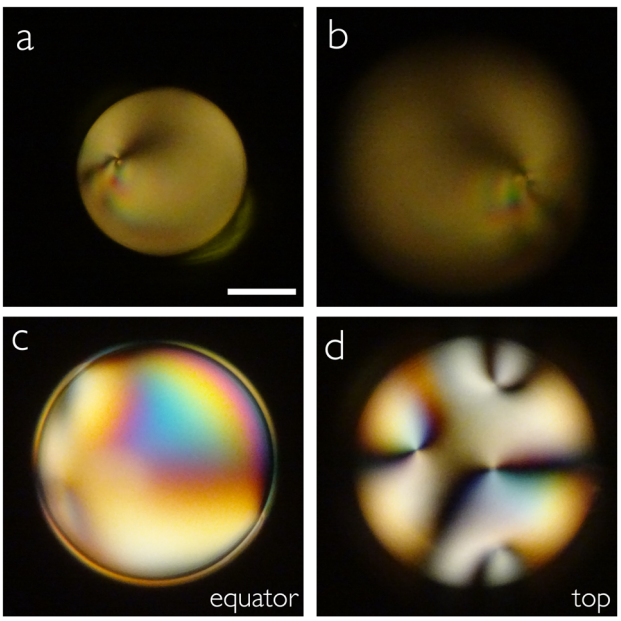

Fig. 6 POM images of a droplet and a shell with 20 wt% 5CB + 80 wt% MPCC mixture at 30 °C. Images (a) and (b) show a droplet with bipolar configuration with the focus on each +1 defect, respectively. Image (c) shows a shell with the focus on the equator and image (d) shows the same shell with the focus on the defect side showing four +1/2 defects. Scale bar represents 50 μm.

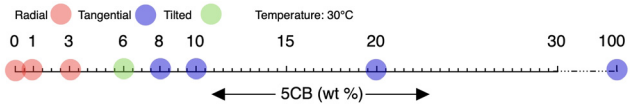

Fig. 7 Graph showing the type of the LC alignments with respect to the 5CB concentration in the 5CB + MPCC mixture.

tangential alignment (a), (b) and the shells show four +1/2 defects near the top (c), (d).

We summarize our observations in Fig. 7, taking 30 °C as a standard reference temperature. Up to 3 wt% 5CB, the director alignment remains normal at the LC–aqueous interface, as for pure MPCC, while above 8 wt% 5CB the alignment is tangential. At the intermediate composition of 6 wt% 5CB, we see the unusual tilted alignment. Concerning stability, we note that shells with 1–3 wt% 5CB as well as shells with 20 wt% or more 5CB are stable over several days, thus enjoying a great stability increase compared to pure MPCC shells. However, for the intermediate 5CB concentrations investigated, 6–10 wt%, the shells are unstable, not much better than those of pure MPCC. This suggests that adding *n*CB to a shell made of an LC that tends to be unstable against water is helpful at concentrations where the director field alignment is well-defined as either normal or tangential, but if an intermediate or undefined alignment results, the stability is poor.

3.5 Does PVA affect the director field configuration?

To see if the presence of PVA has an impact on the unusual alignment of MPCC at an interface to aqueous phases, we end the Results section by comparing pure water with a 10 wt% aqueous PVA solution as bounding phases for droplets of MPCC, 5CB and various mixtures of the two mesogens. While the shell geometry would have been the most interesting, the very low stability of MPCC shells even when using PVA solution as surrounding phases renders it practically impossible to stabilize MPCC shells with pure water as surrounding phases. On the other hand, droplets of MPCC can easily be prepared by stirring with water as continuous phase, and they are stable against coalescence for enough time to study their textures.

In pure water, pure MPCC droplets adopt a normal director field and pure 5CB droplets adopt a tangential director field. Thus, the presence of PVA at 1 wt% concentration used in the experiments above does not influence the alignment of either pure LC compared to when the LC is in contact with pure water. We additionally prepare droplets with 20 and 80 wt% 5CB, respectively, the remainder MPCC, in 10 wt% PVA solution and in pure water, respectively. While the droplets with 80% 5CB are tangential-aligned in both continuous phases (Fig. 8(a) and (b)), we see a difference when the 5CB content is 20%. In this case, the droplets adopt a tangential director field in PVA solution (Fig. 8(c)), as did the shells, but, surprisingly, in pure water the droplets are normally aligned, see Fig. 8(d). Apparently, the balance between tangential and normal alignment of the MPCC + 5CB mixture in contact with water is so subtle that it is affected by the presence of PVA, at least at this high concentration, such that the amount of 5CB required to promote tangential alignment is even higher against pure water than against the 10 wt% aqueous PVA solution.

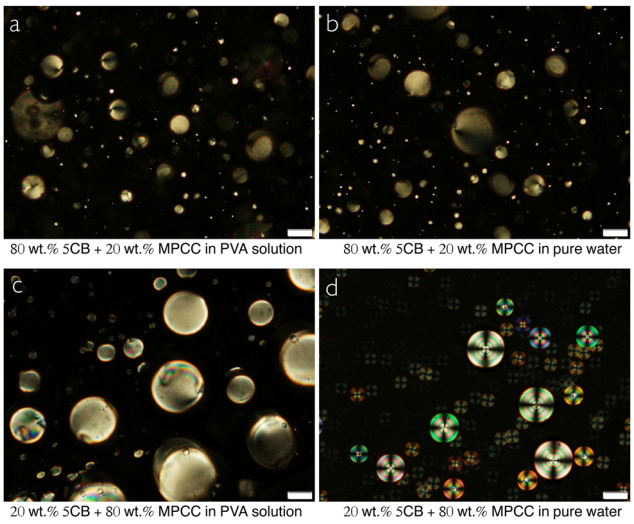

Fig. 8 POM images of droplets made with 80 wt% and 20 wt% 5CB in MPCC, suspended in 10 wt% PVA solution (a), (c) and in pure water (b), (d), respectively. Scale bars represent 50 μm.

4 Discussion

The polar nature of the cyano group and the high polarizability of the aromatic core give cyanobiphenyls their typical high dipole moments μ and high dielectric permittivity $\varepsilon_{\parallel}$ along the director, compared to non-cyano-terminated mesogens like MBBA and MPCC (Table 1). The cyano (nitrile) group is also a good hydrogen bond acceptor while phenyl groups are weak hydrogen bond donors along the perimeter, and acceptors in the center. Starting with the impact of the phenyl rings, it is thus relatively easy to understand that their presence promotes planar alignment. In the choice between being in contact with aliphatic end chains or with aromatic cores, water clearly prefers the latter. Effectively, the hydrogen bonding interaction with the aromatic cores in case of tangential alignment reduces the interfacial tension γ with respect to the van der Waals interaction with aliphatic chains in case of normal alignment.[43]

It is less obvious to explain why non-aromatic mesogens should adopt a normal alignment to water, which is apparently the case as witnessed by the experiments with MPCC shells and droplets in contact with pure water or aqueous PVA solution. Certainly, the interfacial energy to water will be higher than for an aromatic mesogen regardless of alignment, explaining the poor stability of shells of non-aromatic LC, but why would this increase be lower for normal than for tangential alignment? Based on Chandler's discussion of the impact of size of non-hydrogen-bonding inclusions in water,[44] we speculate that the reason may be the greater effective contact area per molecule in case of tangential alignment, enhanced by the presence of cyclohexane rings, compared to normal alignment. While neither orientation allows hydrogen bonds between the water

molecules and the mesogens, the small instantaneous molecular contact area in case of normal alignment could allow water molecules to fluctuate around each alkyl chain terminus to dynamically form a maximum number of hydrogen bonds with each other. Even if they might not reach their full capacity of four hydrogen bonds per water molecule, at least three per molecule should be possible when averaged over time. While this comes at the cost of restricted freedom and hence reduced entropy, it still reduces the free energy compared to sacrificing hydrogen bonds entirely. In case of tangential alignment, in contrast, the larger molecular contact area of the mesogen does not give this option even within the scope of dynamic fluctuations, and water molecules near the LC probably lose hydrogen bonds compared to normal director anchoring. Therefore, tangential alignment would add an enthalpic penalty which increases the free energy of the interface even more. This would explain the preference for normal alignment when no mesogen–water hydrogen bonding is possible at all. We hope that future computer simulations of fluctuating molecules on both sides of the interface in the different scenarios can put this speculation to the test.

To fully appreciate why the mesogen chemical structure is so important in PVA-stabilized emulsions, it is helpful to note that PVA is not a surfactant (Surface Active Agent) in the traditional sense. First, PVA reduces the LC–water interfacial tension γ much less than is typical for surfactants. In a recent study,[43] we measured the interfacial tension of 5CB droplets to aqueous solutions of PVA and of the commonly used surfactant SDS, respectively, extrapolating the data to zero solute concentration to determine γ for tangential and normal director alignment, respectively. For pure water, the interfacial tension is $\gamma_{\parallel} = 30.8$ mN m^{-1} for tangential and $\gamma_{\perp} = 31.9$ mN m^{-1} for normal alignment, the difference (albeit small) explaining the tangential alignment that is normally seen for 5CB in contact with water. While addition of SDS strongly reduces $\gamma_{\perp}$ to about 10 mN m^{-1} at 6 mM SDS, explaining why SDS addition rapidly changes the alignment of 5CB to normal at the LC–aqueous interface, even a very high concentration of PVA (10 wt%) left the interfacial tension at the rather high value of $\gamma_{\parallel} = 28.4$ mN m^{-1}. This is a reduction of only about 8%, to be compared to 67% for the surfactant. The second big difference to traditional surfactants is the polymeric and non-amphiphilic nature of PVA. Even if the 15% non-hydrolyzed monomers afford some variation of hydrophilicity along each molecule chain, the result is a random, not a block copolymer. Its stabilizing effect on LC shells is thus most likely mainly of steric nature, the fully hydrated random PVA coils in the continuous phase preventing two shells from approaching each other to a point where they would risk coalescing. We argue that differences between different LCs observed in this study can therefore be attributed in almost all cases to their different interaction with water. In the one case where we saw a difference between PVA solution and pure water, we used ten times the usual concentration of PVA and we had a mixture where tangential and normal anchoring were very nearly balanced, then allowing the presence of PVA to shift the balance somewhat in favor of tangential alignment.

Our reconfirmation of the stabilizing effect of a small concentration of a cyano-terminated mesogen to shells of LC that on their own are unstable against water can be well understood by considering the good hydrogen bonding capacity of the cyano group, reducing the interfacial tension to water. Given the amphiphilic character of 5CB (or any other *n*CB or *n*OCB mesogen), one may suspect that the 5CB at low concentration acts to some extent as a surfactant when added to an MPCC shell or droplet, adsorbing mainly at the LC–water interface with the cyano group facing the water. This would be perfectly in line with the observed normal alignment of MPCC shells with 1–3 wt% 5CB added.

But why do the shells loose their stability in the range 6–10 wt% 5CB and why do the CCH-5 droplets adopt a tangential director field configuration, given that the mesogen has a non-aromatic core? We believe the reason is the tendency of cyano-terminated mesogens to dimerize in antiparallel configuration to maximize the overlap of aromatic regions of adjacent molecules, even if these comprise only the cyano groups as in CCH-5.[33,34] This means that the mesogen effectively loses its amphiphilic character, as the dimer is mirror symmetric, terminated by an aliphatic chain at each end. Thus, in the case of a pure LC of cyano-terminated mesogens, or in case of a mixture beyond a threshold concentration of such mesogens, they cannot act as surfactants promoting a normal director field at an aqueous interface. Instead, they promote tangential anchoring to maximize water contact with the overlapping cyano groups, as well as aromatic rings when they are present, of the antiparallel dimers. This would perfectly explain the behavior of the MPCC + 5CB mixtures. Up to 3 wt% 5CB, the 5CB molecules are too much in minority to find partners for dimerizing, and they thus act as amphiphilic individual molecules adsorbing at the LC–water interface, stabilizing the shell and promoting a normal director field. But beyond a threshold concentration, which appears to be between 3 and 6 wt%, dimerization starts occurring, and we have competition between dimers promoting tangential alignment and monomers promoting normal alignment. The result is the unusual tilted director field seen in Fig. 4(a) and (b) and a loss in shell stability. Once the concentration of 5CB is high enough for all 5CB molecules to dimerize, they promote tangential alignment and again stabilize the shell. Also this scenario would be very worthwhile to study with computer simulations in a future follow-up study to the experimental work.

5 Conclusions

In summary, the above observations clearly show that the chemical structure of mesogens has a significant importance for how an LC aligns its director field in contact with water, as well as how stable such an interface is. While this should not really be surprising from a fundamental chemical interactions perspective, it nevertheless challenges the commonly prevailing expectation that LC shells are tangential in contact with water, with or without PVA. This expectation has its origin in the fact that almost all prior reports on LC shells used *n*CB mesogens, the few exceptions still using mesogens with aromatic cores. We believe our experiments with MPCC shells are the first example of LC shells comprising entirely non-aromatic mesogens.

Our systematic study of mesogens varying from strongly aromatic to completely aliphatic, with and without cyano group termination, allows us to conclude that the aromaticity is key to promoting tangential alignment to aqueous phases, while the cyano group termination is very effective in increasing the stability of an LC–aqueous interface. We also find that a small amount of cyanobiphenyl mesogen is very effective in stabilizing LC shells without impacting their alignment compared to that of the pure LC shell, but already at a concentration of a few percent, the stabilizing effect may be lost, most likely because the cyanobiphenyl mesogens then start dimerizing. We would greatly welcome follow-up computer simulation studies to test the suggestions made in this work based on our experimental findings.

Conflicts of interest

There are no conflicts to declare.

Acknowledgements

This research was funded by the Luxembourg National Research Fund (FNR), grant references C20/MS/14771094 (ECLIPSE) and 2016/10935404 (doctoral training grant PRIDE MASSENA). For the purpose of open access, the authors have applied a Creative Commons Attribution 4.0 International (CC BY 4.0) license to any Author Accepted Manuscript version arising from this submission.

Notes and references

1 T. Lopez-Leon and A. Fernandez-Nieves, *Colloid Polym. Sci.*, 2011, **289**, 345–359.
2 M. Urbanski, C. G. Reyes, J. Noh, A. Sharma, Y. Geng, V. S. R. Jampani and J. P. Lagerwall, *J. Phys.: Condens. Matter*, 2017, **29**, 133003.
3 T. Lopez-Leon, V. Koning, K. B. S. Devaiah, V. Vitelli and A. Fernandez-Nieves, *Nat. Phys.*, 2011, **7**, 391–394.
4 M. Sadati, Y. Zhou, D. Melchert, A. Guo, J. Martinez-Gonzalez, T. Roberts, R. Zhang and J. de Pablo, *Soft Matter*, 2017, **13**, 7465–7472.
5 B. Hokmabad, K. Baldwin, C. Krüger, C. Bahr and C. Maass, *Phys. Rev. Lett.*, 2019, **123**, 178003.
6 Y. Ishii, Y. Zhou, K. He, Y. Takanishi, J. Yamamoto, J. de Pablo and T. Lopez-Leon, *Soft Matter*, 2020, **16**, 8169–8178.
7 J. Noh, Y. Wang, H.-L. Liang, V. S. R. Jampani, A. Majumdar and J. P. F. Lagerwall, *Phys. Rev. Res.*, 2020, **2**, 033160.
8 J. Noh and J. P. Lagerwall, *Crystals*, 2021, **11**, 913.
9 G. Napoli and L. Vergori, *Phys. Rev. E*, 2021, **104**, L022701.
10 S. Seyednejad and M. Mozaffari, *Phys. Rev. E*, 2021, **104**, 014701.
11 K. He, Y. Zhou, H. Ramezani-Dakhel, J. de Pablo, A. Fernandez-Nieves and T. Lopez-Leon, *Soft Matter*, 2022, **18**(7), 1395–1403.
12 C. de Araújo, E. de Oliveira, M. Lyra, L. Mirantsev and I. de Oliveira, *Soft Matter*, 2022, **18**, 4189–4196.
13 L. Carenza, G. Gonnella, D. Marenduzzo, G. Negro and E. Orlandini, *Phys. Rev. Lett.*, 2022, **128**, 027801.
14 A. Sharma and J. P. F. Lagerwall, *Liq. Cryst.*, 2018, **45**, 2319–2328.
15 A. Sharma, D. Gupta, G. Scalia and J. P. F. Lagerwall, *Phys. Rev. Res.*, 2022, **4**, 013130.
16 S. Park, S. Lee and S. Kim, *Adv. Mater.*, 2020, **32**, e2002166.
17 Y. Geng, J.-H. Jang, K.-G. Noh, J. Noh, J. P. Lagerwall and S.-Y. Park, *Adv. Opt. Mater.*, 2018, **6**, 1700923.
18 N. Popov and J. P. F. Lagerwall, *Front. Soft Matter*, 2022, **2**, 991375.
19 E.-K. Fleischmann, H.-L. Liang, N. Kapernaum, F. Giesselmann, J. P. F. Lagerwall and R. Zentel, *Nat. Commun.*, 2012, **3**, 1178.
20 A. Sharma, A. M. Stoffel and J. P. F. Lagerwall, *J. Appl. Phys.*, 2021, **129**, 174701.
21 Y. Iwai, T. Maeda, Y. Uchida, F. Araoka and N. Nishiyama, *Adv. Photonics Res.*, 2021, **2**, 2000079.
22 J. Kang, S. Kim, A. Fernandez-Nieves and E. Reichmanis, *J. Am. Chem. Soc.*, 2017, **139**, 5708–5711.
23 M. Schwartz, G. Lenzini, Y. Geng, P. Rønne, P. Ryan and J. Lagerwall, *Adv. Mater.*, 2018, **30**, 1707382.
24 L. Tran and K. Bishop, *ACS Nano*, 2020, **14**, 5459–5467.
25 H. Agha, Y. Geng, X. Ma, D. I. AvÅŸar, R. Kizhakidathazhath, Y.-S. Zhang, A. Tourani, H. Bavle, J.-L. Sanchez-Lopez and H. Voos, *et al.*, *Light: Sci. Appl.*, 2022, **11**, 309.
26 I.-S. Heo and S.-Y. Park, *Sens. Actuators, B*, 2017, **251**, 658–666.
27 S. Lee, H. Seo, Y. Kim and S. Kim, *Adv. Mater.*, 2017, **29**, 1606894.
28 J.-G. Kim and S.-Y. Park, *Adv. Opt. Mater.*, 2017, **5**, 1700243.
29 D. Myung and S. Park, *ACS Appl. Mater. Interfaces*, 2019, **11**, 20350–20359.
30 Y. Geng, R. Kizhakidathazhath and J. P. F. Lagerwall, *Adv. Funct. Mater.*, 2021, **31**, 2100399.
31 M. H. Peter and J. Collings, *Introduction to Liquid Crystals: Chemistry and Physics*, CRC Press, 1997.
32 S. Pestov and V. Vill, in *Springer Handbook of Condensed Matter and Materials Data*, ed. W. Martienssen and H. Warlimont, Oxford University Press, 2005, pp. 941–978.
33 M. R. Wilson and D. A. Dunmur, *Liq. Cryst.*, 1989, **5**, 987–999.
34 D. A. Dunmur and K. Toriyama, *Liq. Cryst.*, 1986, **1**, 169–180.
35 A. Fernandez-Nieves, V. Vitelli, A. Utada, D. R. Link, M. Marquez, D. R. Nelson and D. A. Weitz, *Phys. Rev. Lett.*, 2007, **99**, 157801.
36 T. Lopez-Leon and A. Fernandez-Nieves, *Phys. Rev. E: Stat., Nonlinear, Soft Matter Phys.*, 2009, **79**, 021707.
37 G. Durey, Y. Ishii and T. Lopez-Leon, *Langmuir*, 2020, **36**, 9368–9376.
38 K. Flatischler, L. Komitov, S. T. Lagerwall, B. Stebler and A. Strlgazzi, *Mol. Cryst. Liq. Cryst.*, 1991, **198**, 119–130.
39 K. R. Amundson and M. Srinivasarao, *Phys. Rev. E: Stat. Phys., Plasmas, Fluids, Relat. Interdiscip. Top.*, 1998, **58**, 1211–1214.
40 G. Volovik and O. Lavrentovich, *Zh. Eksp. Teor. Fiz.*, 1983, **85**, 1159–1166.
41 H.-L. Liang, E. Enz, G. Scalia and J. Lagerwall, *Mol. Cryst. Liq. Cryst.*, 2011, **549**, 69–77.
42 H.-L. Liang, R. Zentel, P. Rudquist and J. Lagerwall, *Soft Matter*, 2012, **8**, 5443–5450.
43 L. Honaker, A. Sharma, A. Schanen and J. Lagerwall, *Crystals*, 2021, **11**, 687.
44 D. Chandler, *Nature*, 2005, **437**, 640–647.